

# Effects of Electric Current and Sample Orientation on Flame Spread over Electrical Wires

Zhao L.Y.<sup>1</sup>, Zhang Q.X.<sup>1</sup>, Tu R.<sup>2</sup>, Fang J.<sup>1</sup>, Wang J.J.<sup>1</sup>, Zhang Y.M.<sup>1,\*</sup>

<sup>1</sup> State Key Laboratory of Fire Science, University of Science and Technology of China, Hefei, Anhui 230026, China

<sup>2</sup> College of Mechanical Engineering and Automation, Huaqiao University, Xiamen, Fujian 361021, China

\*Corresponding author's email: [zhangym@ustc.edu.cn](mailto:zhangym@ustc.edu.cn)

## ABSTRACT

Experiments were performed to study the effects of electric current and sample orientation on flame spread along the polyethylene (PE) insulation on copper wires. The flame spread rate vs. inclination angle showed a non-monotonic trend i.e., flame spread rate first decreased and then increased as the inclination angle increased. The molten polymer coating flew along the wire during the spread if the wire was inclined. For upward flame spread, a periodic flame spread phenomenon was observed due to the flowing of molten polymer. A sub-flame was observed to spread in the opposite direction to the primary flame. The flowing of molten insulation has little influence on upward flame spread rate. With the increase of the electric current, both the amount of molten insulation and the flame spread rate increased. The downward spread was shown to be more susceptible to the electric current in this study. For downward flame spread, the flowing molten polymer brought heat from the burning region to the preheat region and promoted the flame spread. A flame spread model concerning with both the orientation angle and electric current was developed in this study.

**KEYWORDS:** Flame spread, electric wire, orientation effect, molten insulation.

## NOMENCLATURE

$c$	constant pressure specific heat (J/(kg·K))	$\rho'$	electrical resistivity ( $\Omega \cdot m$ )
$\bar{h}$	average convection coefficient (W/(m <sup>2</sup> ·K))	$\alpha$	thermal diffusivity (m <sup>2</sup> /s)
$\Delta H$	latent heat of pyrolysis (J/kg)	$\beta$	volumetric thermal expansion coefficient (K <sup>-1</sup> )
$I$	constant electric current (A)	$\lambda$	thermal conductivity (W/(m·K))
$L_f$	flame length (cm)	$\varepsilon$	emissivity (-)
$L_h$	flame preheat length (cm)	$\nu$	kinematic viscosity (m <sup>2</sup> /s)
$L_p$	pyrolysis length (cm)	$\sigma$	Stefan-Boltzmann constant (W/(m <sup>2</sup> ·K <sup>4</sup> ))
$Nu$	Nusselt number (-)	$\phi$	inclination angle (grad)
$Q$	heat flux (W)	$\Phi$	Joule heat (W)
$q''$	heat flux per unit area (W/m <sup>2</sup> )		
$r$	radius (cm)		
$Ra$	Rayleigh number		
$T$	temperature (K)		

### Subscripts

$a$	ambient
$c$	core
$f$	flame

Proceedings of the Ninth International Seminar on Fire and Explosion Hazards (ISFEH9), pp. 786-795

Edited by Snegirev A., Liu N.A., Tamanini F., Bradley D., Molkov V., and Chaumeix N.

Published by Saint-Petersburg Polytechnic University Press

ISBN: 978-5-7422-6498-9 DOI: 10.18720/spbpu/2/k19-54

$t$	time (s)	$g$	gas
$V_f$	flame spread rate (cm/s)	$p$	polymer coating or pyrolysis
<b>Greek</b>		0	Original
$\rho$	density (kg/m <sup>3</sup> )		

## INTRODUCTION

Flame spread along the polymeric coatings on electrical wires is of interest for fire prevention and has been widely studied in recent years [1-3]. Fujita et al. performed a series of experiments to study the effects of external flow velocity [1], wire size [2], ambient pressure [3] and oxygen concentration [4] on flame spread over polyethylene (PE) wires in microgravity. Takahashi et al. [5] studied the influence of external flow velocity on the volume change of the melted insulation in microgravity. Huang et al. [6] developed a model to explain the ignition and ignition-to-spread phenomenon of electrical wires.

Previous studies usually considered the burning of horizontal wires, and limited studies were on the orientation effect. However, in practical application, flame spread over wires occurs at many different orientation angles. Hu et al. [7] studied the limiting oxygen concentration for extinction of upward spreading flames over inclined wires with opposed-flow. Lu et al. [8] studied the interaction between the wire inclination and horizontal wind. Hu et al. [9] found that as the inclination angle  $\phi$  varies from  $-90^\circ$  to  $+75^\circ$  (relative to the horizontal plane, ‘-’ means downward spread and ‘+’ means upward spread), the flame spread rate (FSR) of electrical wires first decreases then increases (‘U’ shape), which is quite different from low thermal conductivity materials such as paper [10] or wood [11]. Explanations of this phenomenon are that for electrical wires with high thermal conductivity metal cores (such as Cu), heat conduction through the metal core from the burning zone to pyrolysis zone dominates the flame spread process, while for low thermal conductivity materials, heat conduction through the solid media could be neglected.

However, it has been found by Yoshinari et al. [12, 13] that for vertical wires, the downward FSR is dominated by the downward dripping of the molten insulation, but is comparatively not sensitive to the core material. During the flame spread process, the polymeric coating first melts, and then decomposes to release combustible gases for burning. If the polymeric coating melts faster than its burning, the molten insulation begins to accumulate and flows along the wire (if the wire is inclined) or drip down (if the wire is horizontal). The phase change process has been numerically analyzed by Kim et al. [14, 15]. Wang et al. [16] found that the accumulation rate of molten insulation increases with the increasing current. Therefore, the effects of flowing molten insulation on wire fire should be concerned especially for cases with large current. When predicting the FSR, Hu et al. [9] neglected the heat flux from the flame to the preheat region ahead of the pyrolysis front in the energy balance equation of wire burning. However, surface heat flux in the preheat zone is very important for flame spread, especially for upward flame spread. In addition, the orientation angle was not included in the model of Hu et al. [9].

In this study, the effects of direct current  $I$  ( $0 \sim 7$  A) and inclination angle  $\phi$ , ( $-90^\circ \sim +60^\circ$ ) on flame spread over PE insulated copper wires were studied. A periodic spread phenomenon was observed in upward flame spread due to the flowing of molten insulation. A flame spread model concerning with electric current and orientation angle was developed.

## EXPERIMENTAL

A schematic drawing of the experimental apparatus is shown in Fig. 1, which mainly consists of a rotary stand, a sample holder, an ignition part and two constant current sources (CCS). PE insulated copper wires (inner diameter:  $d_c = 0.5$  mm and outer diameter:  $d_p = 0.8$  mm) were used as samples in the tests. The copper wires were applied with constant currents from 0 to 7 A by CCS 1 with a precision of 0.1 A. And a coil heater (NiCr) located at one end of the sample wire was charged with 6 A current by CCS 2 for ignition. A weight coupled with a pulley fixed on the sample holder was used to keep the sample straight during the experiments. A protractor was used to accurately set the angle of wire  $\phi$  (relative to the horizontal plane, ‘-’ means downward spread and ‘+’ means upward spread) ranging from  $-90^\circ$  to  $+60^\circ$ . During the experiments, a side-view video camera (SONY NEX-5R, 30fps) was used to record the flame spread process. The characteristic parameters of flame shape and propagation velocity were obtained by image processing algorithm.

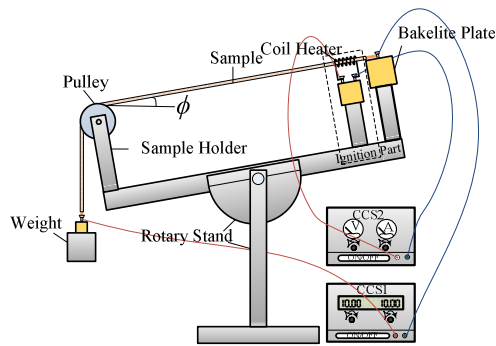


**Fig. 1.** Flame spread apparatus.

In the tests, the sample wire was ignited after being energized for 3 minutes (to make the sample wire reach a relative thermal equilibrium). Once ignition occurred, the ignition current was cut off immediately, while the electric current in the sample wire was still on. Effective length of the sample wire was 25 cm (distance from the ignition point to the pulley). Each test condition was repeated at least three times to ensure reproducible results. All experiments were performed under laboratory conditions of approximately  $20 \pm 1^\circ\text{C}$  and  $30 \pm 5\%$  relative humidity.

## RESULTS AND DISCUSSION

### Periodic flame spread phenomenon

During the flame spread, the insulation melts, flows into the burning region and accumulates into a ball. When the ball is large enough, part of it flows down along the inclined wire. For downward flame spread ( $\phi < 0$ ), part of the molten ball flows down from the burning zone to the preheat zone, losing heat to the preheat fuel and is not burnt. However, for upward flame spread ( $\phi > 0$ ), a periodic spread phenomenon is observed. In Fig. 2, variations of the flame shape with time in one cycle of the periodic spread phenomenon for  $\phi = +15^\circ$  are shown. As the molten ball flows along the wire, it remains burning and consumes gradually, which results in the appearance of a subflame downstream. Height of the primary flame decreases first because of the flowing down of molten liquid, and then recovers itself as the flame continues to melt the unburnt fuel. The sub-flame moves in the opposite direction to the primary one. It decreases in size with time as the molten ball consumes gradually. In Fig. 2b, it is seen that the flame even breaks off (1.40s) with  $I = 3$  A.

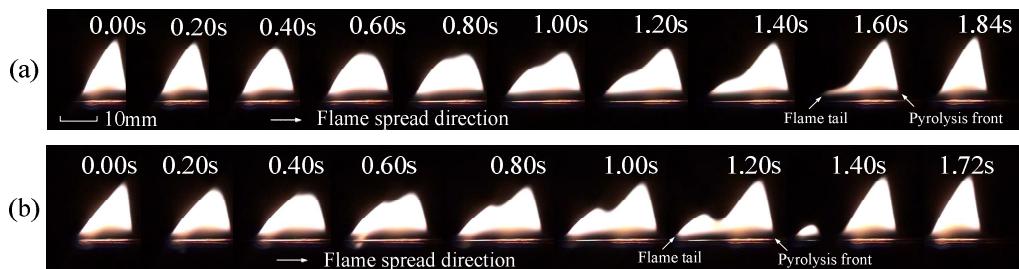


**Fig. 2.** Variations of flame shape with time at  $\phi = +15^\circ$  with (a)  $I = 0$  A and (b)  $I = 3$  A.

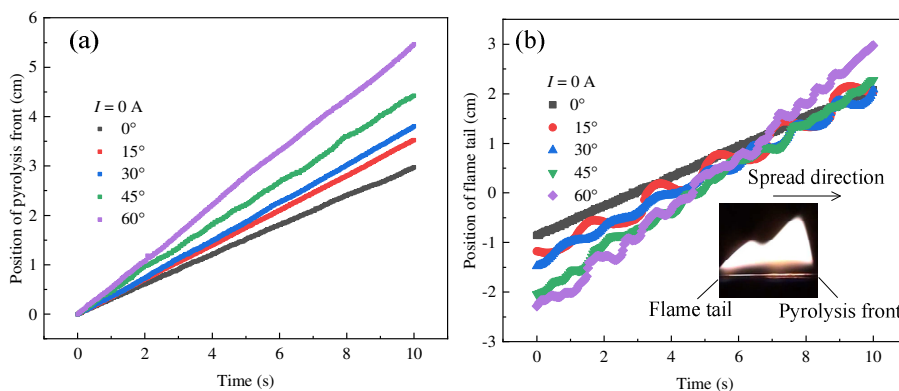


**Fig. 3.** Propagation of (a) pyrolysis front and (b) flame tail with time at  $I = 0$  A in upward spread.

Figs. 3a and 3b illustrate the propagation of pyrolysis front and flame tail as a function of time with different orientation angle at  $I = 0$  A in upward flame spread. The flame tail moves periodically with time and the cycle is shorter for the larger orientation angle. The pyrolysis front moves linearly with time and is shown not to be affected by the flame tail. In this study, the average movement rate of pyrolysis front is taken as flame spread rate (FSR). Note that for upward flame spread, though the flame shape varies periodically, structure of the primary flame just before the sub-flame appears is used for model prediction of flame spread hereinafter.

### Flame shape and flame spread rate

Figure 4 shows the variations of flame length  $L_f$  and pyrolysis length  $L_p$  with inclination angles. Definitions of flame length and pyrolysis length are given in Fig. 4a. Length of the wire surrounded by the flame is defined as pyrolysis length. One can see that both  $L_f$  and  $L_p$  first decrease and then increase as the inclination angle increases from  $-90^\circ$  to  $+60^\circ$ , which shows a “U” trend as is described in the work of Hu et al [9]. The smallest values of  $L_f$  and  $L_p$  appear at  $\phi = 0$ . As the current increases, both the flame length and pyrolysis length increase. In Fig. 4a, as the electric current increases, the flame length data of downward spread are more scattered than that of the upward case, which indicates that the electric current has a stronger effect on flame length in downward spread.

Flame spread rate as a function of inclination angle is plotted in Fig. 5. The dependences of FSR on inclination angle and electrical current are similar to that of the flame length. The FSR varies with the inclination angle as a “U” trend. The FSR data of different currents are more scattered for downward spread indicating that the electric current has a stronger effect on downward FSR than upward FSR. The primary reasons are explained as follows. As the electrical current increases, the

polymeric coating melts faster and more molten insulation flows along the wire if the wire is inclined. The FSR depends more strongly on the heat flux to the surface in the preheat zone than on the surface heat flux in the burning zone [17]. For upward flame spread, the molten insulation brings heat to the burning zone, while for downward spread, the molten insulation brings heat to the preheat zone and makes greater contributions to flame spread.

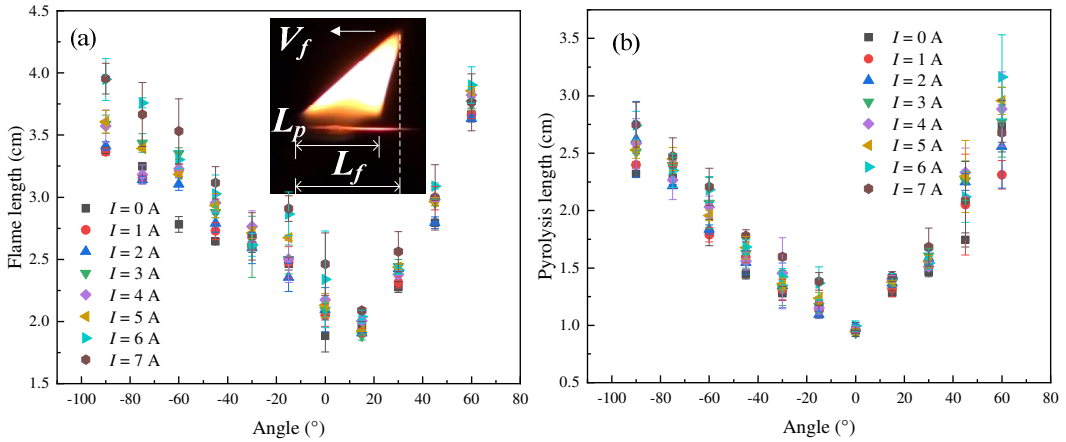


Fig. 4. Variations of (a) flame length and (b) pyrolysis length with inclination angle.

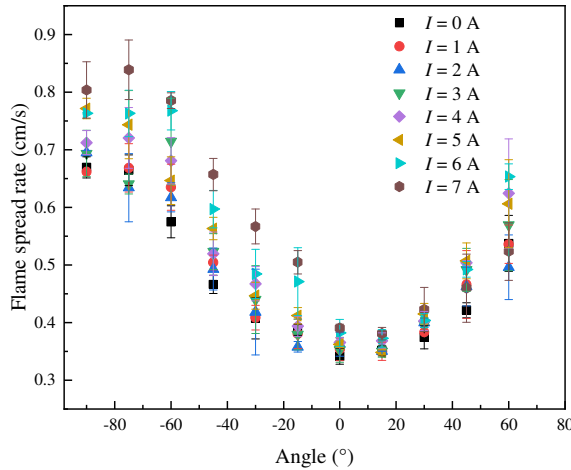


Fig. 5. Flame spread rate as a function of the inclination angle.

Both flame length and pyrolysis length are characteristic lengths that are related to the heat transfer process from the flame to the wire. Heat balance analyses concerning with the two characteristic lengths, orientation angle and electric current are conducted in the next section to predict the FSR.

### Flame spread model

A simplified description of steady-state flame spread over a thin electrical wire at a constant velocity of  $V_f$  is illustrated in Fig. 6. Several assumptions are adopted here: (1) the coordinate system is fixed to the location of the flame; (2) both the PE insulation and core wire are thermally thin so that temperature profile across the cross-section of PE or metal core is uniform; (3) heat conduction

through the PE insulation is ignored; (4) the complex shape change of polymer during the melting process is ignored; (5) flame radiation heat feedback is ignored; (6) heat flux from the molten insulation to the wire is ignored.

After being energized for 3 min before ignition, temperature of the wire reaches steady state, which gives:

$$I^2 \frac{\rho'}{\pi r_c^2} - 2\pi r_p \bar{h}_1 (T_0 - T_a) = 0, \quad (1)$$

where  $r$  is radius, with the subscript  $c$  for core and  $p$  for polymer coating,  $\rho'$  is the electrical resistivity,  $T_a$  is the ambient temperature,  $T_0$  is the thermal equilibrium temperature of the wire before ignition and  $\bar{h}$  is the average convection coefficient over the wire surface. Then we obtain

$$T_0 = T_a + \frac{\rho' I^2}{(2\pi r_p) \bar{h}_1 (\pi r_c^2)}. \quad (2)$$

$\bar{h}$  can be calculated as follow [18]:

$$\bar{h} = \bar{N}u_d \lambda_g / d = (C R a_d^n) \lambda_g / d, \quad (3)$$

$$R a_d = G r_d P r = \frac{g \beta (T - T_a) d^3 |\sin \phi|}{\nu^2},$$

where  $\lambda_g$  is the thermal conductivity of gas,  $\beta$  is the volumetric thermal expansion coefficient,  $\nu$  is the kinematic viscosity,  $C = 1.02$ , and  $n = 0.148$ .

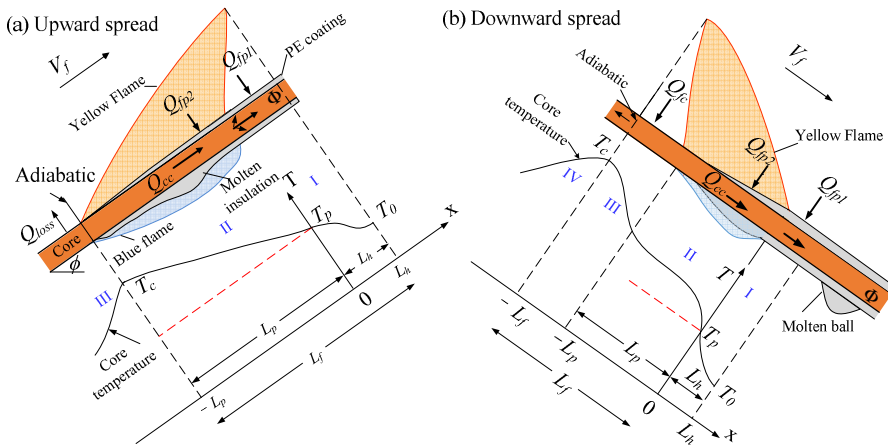


**Fig. 6.** Illustration of the flame structure and temperature profile of wire during steady-state spread: (a) upward spread, and (b) downward spread.

Equations of heat transfer between flame and wire can be expressed as:

$$Q_{in} + \Phi = \pi (r_p^2 - r_c^2) \rho_p V_f [c_p (T_p - T_0) + \Delta H] + \pi r_c^2 \rho_c c_c V_f (T_c - T_0), \quad (4)$$

where  $Q_{in}$  is the incident heat flux from flame to wire,  $c$  is the heat capacity,  $T_c$  is the temperature of copper wire at the flame tail,  $\Delta H$  is the latent heat of pyrolysis of the polymer coating (254 kJ/kg for PE [9]), and  $\Phi$  is the Joule heat produced in the control volume expressed as:

$$\Phi = I^2 \frac{\rho'}{\pi r_c^2} L_{ch}, \quad (5)$$

where  $L_{ch}$  is the length of the control volume. Then the FSR can be obtained from Eq. (4) as:

$$V_f = \frac{Q_{in} + \Phi}{\pi(r_p^2 - r_c^2)\rho_p [c_p(T_p - T_0) + \Delta H] + \pi r_c^2 \rho_c c_c (T_c - T_0)}, \quad (6)$$

### Upward flame spread

For upward spread (as shown in Fig. 6a), the incident heat flux from flame to wire is:

$$Q_{in} = Q_{fp1} + Q_{fp2}, \quad (7)$$

where  $Q_{fp1}$ ,  $Q_{fp2}$  are the heat convection between flame and polymer coating in the preheat zone (Region I in Fig. 6a) and the pyrolysis zone (Region II in Fig. 6a), respectively

The heat flux per unit area from flame to wire can be expressed as [19]:

$$\dot{q}''(x) = \begin{cases} \dot{q}''(0)\exp(-x/L_h), & x > 0 \\ \dot{q}''(0), & -L_p < x < 0 \end{cases}, \quad (8)$$

where  $L_h$  is the flame preheat length expressed as  $L_h = L_f - L_{ba}$ , and  $\dot{q}''(0)$  is the surface heat flux per unit area at  $x = 0$ , which can be estimated as:

$$\dot{q}''(0) \approx \bar{h}_2 (T_f - T_p), \quad (9)$$

where  $\bar{h}_2$  is the average heat transfer coefficient over the wire surface in Region II. We can see from Eqs. (3) and (9) that as the inclination angle increases,  $\bar{h}$  increases and therefore  $\dot{q}''(0)$  increases.

In the preheat region,  $Q_{fp1}$  can be expressed as:

$$Q_{fp1} = 2\pi r_p \int_0^\infty \dot{q}''(0)\exp(-x/L_h)dx = 2\pi r_p L_h \dot{q}''(0). \quad (10)$$

In Region II,

$$Q_{fp2} = 2\pi r_p L_p \dot{q}''(0). \quad (11)$$

At the flame tail, thickness of the molten insulation reduces to zero and the wire core is exposed to the flame. In Region III (as shown in Fig. 6a), heat flux from the flame is negligible and temperature of the wire core decreases rapidly due to heat loss to the environment. Therefore, it's reasonable to assume that temperature of the wire reaches the maximum at the flame tail, and then  $T_c$  can be determined by

$$\dot{q}''(0) + I^2 \rho' / \pi r_c^2 (2\pi r_c) = \varepsilon \sigma (T_c^4 - T_a^4) + \bar{h}_3 (T_c - T_a) \quad (12)$$

By substituting Eqs. (5), (10) and (11) in Eq. (6), upward FSR can be predicted as:

$$V_f = \frac{(2\pi r_p \dot{q}''(0) + I^2 \rho' / \pi r_c^2) L_f}{\pi (r_p^2 - r_c^2) \rho_p [c_p (T_p - T_0) + \Delta H] + \pi r_c^2 \rho_c c_c (T_c - T_0)}. \quad (13)$$

### Downward flame spread

For downward flame spread (Fig. 6b), the incident heat flux from flame to wire  $Q_{in}$  is:

$$Q_{in} = Q_{fp1} + Q_{fp2} + Q_{fc}, \quad (14)$$

where  $Q_{fc}$  is the heat flux from flame to exposed wire in Region III (in Fig. 6b). The heat flux per unit area from flame to wire can be expressed as:

$$\dot{q}''(x) = \dot{q}''(0) \begin{cases} \exp(-x/L_h), & x > 0 \\ 1, & -L_p < x < 0, \\ \exp(-(x+L_p)/L_p), & x < -L_p \end{cases} \quad (15)$$

where  $L_h$  is the flame preheat length approximated as [20]:

$$L_h \approx \sqrt{2\alpha_g} / u_\infty \approx \sqrt{2\alpha_g} / (\alpha_g g \sin|\phi|)^{1/3}, \quad (16)$$

where  $\alpha_g$  is the thermal diffusivity of gas.

Heat fluxes from flame to wire are:

Region I:

$$Q_{fp1} = 2\pi r_p \int_0^\infty \dot{q}''(0) \exp(-x/L_h) dx = 2\pi r_p L_h \dot{q}''(0), \quad (17)$$

Region II:

$$Q_{fp2} = 2\pi r_p L_p \dot{q}''(0), \quad (18)$$

Region III:

$$Q_{fc} = 2\pi r_c \int_{-L_f}^{-L_p} \dot{q}''(0) \exp((x+L_p)/L_p) dx = 2\pi r_c L_p \dot{q}''(0) (1 - \exp(1 - L_f/L_p)) \quad (19)$$

Temperature of the copper core reaches the maximum at  $x = -L_f$ , and  $T_c$  can be determined by:

$$\dot{q}''(0) \exp((-L_f + L_p)/L_p) + I^2 \rho' / \pi r_c^2 (2\pi r_c) = \varepsilon \sigma (T_c^4 - T_a^4) + \bar{h}_3 (T_c - T_a) \quad (20)$$

By substituting Eqs. (14) and (17)-(19) into Eq. (6), the downward FSR can be predicted by:

$$V_f = \frac{2\pi r_p (L_p + L_h) \dot{q}''(0) + 2\pi r_c L_p (1 - \exp(1 - L_f/L_p)) \dot{q}''(0) + I^2 \rho' (L_f + L_h) / \pi r_c^2}{\pi (r_p^2 - r_c^2) \rho_p [c_p (T_p - T_0) + \Delta H] + \pi r_c^2 \rho_c c_c (T_c - T_0)} \quad (21)$$

The predicted flame spread rates under various conditions are obtained by deriving characteristic lengths into Eq. (13) or (21), which are plotted in Fig. 7. Gas phase properties are all evaluated at



the film temperature. It is observed that for opposed-flow flame spread, the predicted values are much smaller than the experimental ones, which is primarily attributed to that flame radiation feedback and heat flux from the molten material (liquid-phase Marangoni convection and dripping heating) are ignored in the model. For upward flame spread, our model achieves a good accuracy. As  $\phi$  increases, the flame sheet moves closer to the sample wire, the flame length elongates and results in a larger heat flux from flame to fuel, which finally leads to a larger FSR as suggested by Eq. (13).

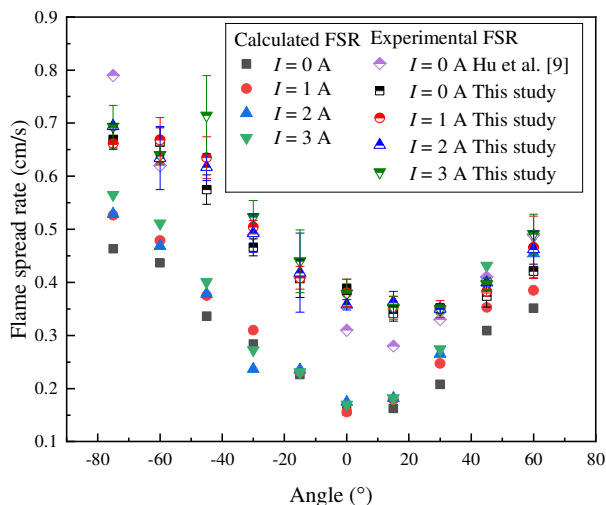


Fig. 7. Comparison of calculated flame spread rate with experimental values.

## CONCLUSIONS

Effects of constant electric current and orientation angle on flame spread over PE insulated copper wires were studied in this paper. The flame spread rate was shown to increase with the increasing electric current. The current had a larger influence on downward flame spread compared with upward spread. For downward spread, the flowing molten liquid brought heat from the burning zone to preheat zone and promoted the spread. For upward flame spread, a periodic flame spread phenomenon was observed due to the flowing of molten polymer. A flame spread model concerning with both the orientation angle and electric current was developed. Good accuracy was observed between the calculated and experimental flame spread rate.

## ACKNOWLEDGMENTS

This work was supported by the National Key Research and Development Plan under Grant No. 2017YFC0805100, the National Natural Science Foundation of China under Grant No. U1733126 and 41675024, and the Fundamental Research Funds for the Central Universities under Grant No. WK2320000035. The authors gratefully acknowledge all of these supports.

## REFERENCES

- [1] O. Fujita, K. Nishizawa, K. Ito, Effect of Low External Flow on Flame Spread over Polyethylene-Insulated Wire in Microgravity, Proc. Combust. Inst. 29 (2002) 2545-2552.

- [2] O. Fujita, M. Kikuchi, K. Ito, K. Nishizawa, Effective Mechanisms to Determine Flame Spread Rate over Ethylene-Tetrafluoroethylene Wire Insulation: Discussion on Dilution Gas Effect Based on Temperature Measurements, *Proc. Combust. Inst.* 28 (2000) 2905-2911.
- [3] Y. Nakamura, N. Yoshimura, H. Ito, K. Azumaya, O. Fujita, Flame Spread over Electric Wire in Sub-Atmospheric Pressure, *Proc. Combust. Inst.* 32 (2009) 2559-2566.
- [4] M. Kikuchi, O. Fujita, K. Ito, A. Sato, T. Sakuraya, Experimental Study on Flame Spread over Wire Insulation in Microgravity, *Proc. Combust. Inst.* 27 (1998) 2507-2514.
- [5] S. Takahashi, H. Takeuchi, H. Ito, Y. Nakamura, O. Fujita, Study on Unsteady Molten Insulation Volume Change During Flame Spreading over Wire Insulation in Microgravity, *Proc. Combust. Inst.* 34 (2013) 2657-2664.
- [6] X. Huang, Y. Nakamura, F.A. Williams, Ignition-to-Spread Transition of Externally Heated Electrical Wire, *Proc. Combust. Inst.* 34 (2013) 2505-2512.
- [7] L. Hu, Y. Lu, K. Yoshioka, Y. Zhang, C. Fernandez-Pello, S.H. Chung, O. Fujita, Limiting Oxygen Concentration for Extinction of Upward Spreading Flames over Inclined Thin Polyethylene-Insulated Nitr Electrical Wires with Opposed-Flow under Normal-and Micro-Gravity, *Proc. Combust. Inst.* 36 (2017) 3045-3053.
- [8] Y. Lu, X. Huang, L. Hu, C. Fernandez-Pello, The Interaction between Fuel Inclination and Horizontal Wind: Experimental Study Using Thin Wire, *Proc. Combust. Inst.* (2018).
- [9] L. Hu, Y. Zhang, K. Yoshioka, H. Izumo, O. Fujita, Flame Spread over Electric Wire with High Thermal Conductivity Metal Core at Different Inclinations, *Proc. Combust. Inst.* 35 (2015) 2607-2614.
- [10] J.G. Quintiere, The Effects of Angular Orientation on Flame Spread over Thin Materials, *Fire Safety J.* 36 (2001) 291-312.
- [11] Y. Zhang, J. Ji, Q. Wang, X. Huang, Q. Wang, J. Sun, Prediction of the Critical Condition for Flame Acceleration over Wood Surface with Different Sample Orientations, *Combust. Flame* 159 (2012) 2999-3002.
- [12] Y. Kobayashi, Y. Konno, X. Huang, S. Nakaya, M. Tsue, N. Hashimoto, O. Fujita, C. Fernandez-Pello, Effect of Insulation Melting and Dripping on Opposed Flame Spread over Laboratory Simulated Electrical Wires, *Fire Saf. J.* 95 (2018) 1-10.
- [13] Y. Kobayashi, X. Huang, S. Nakaya, M. Tsue, C. Fernandez-Pello, Flame Spread over Horizontal and Vertical Wires: The Role of Dripping and Core, *Fire Saf. J.* 91 (2017) 112-122.
- [14] Y. Kim, A. Hossain, Y. Nakamura, Numerical Study of Melting of a Phase Change Material (Pcm) Enhanced by Deformation of a Liquid-Gas Interface, *Int. J. Heat Mass Transfer* 63 (2013) 101-112.
- [15] Y. Kim, A. Hossain, Y. Nakamura, Numerical Modeling of Melting and Dripping Process of Polymeric Material Subjected to Moving Heat Flux: Prediction of Drop Time, *Proc. Combust. Inst.* 35 (2015) 2555-2562.
- [16] H. He, Q. Zhang, R. Tu, L. Zhao, J. Liu, Y. Zhang, Molten Thermoplastic Dripping Behavior Induced by Flame Spread over Wire Insulation under Overload Currents, *J. Hazard. Mater.* 320 (2016) 628-634.
- [17] M. Sibulkin, J. Kim, J.V. Creeden Jr., The Dependence of Flame Propagation on Surface Heat Transfer I. Downward Burning, *Combust. Sci. Technol.* 14 (1976) 43-56.
- [18] V.T. Morgan. The Overall Convective Heat Transfer from Smooth Circular Cylinders, In: *Advances in Heat Transfer*, Elsevier, 1975, pp. 199-264.
- [19] M. Sibulkin, J. Kim, The Dependence of Flame Propagation on Surface Heat Transfer II. Upward Burning, *Combust. Sci. Technol.* 17 (1977) 39-49.
- [20] J.G. Quintiere, *Fundamentals of Fire Phenomena*. John Wiley, Chichester, 2006, pp. 210-211.